Indian Journal of Chemistry
Vol. 64, April 2025, pp. 427-433
DOI: 10.56042/ijc.v64i4.17376

A comparative study on electrochemical performance of GC/MFe_2O_4 (M = Cu and Ni) electrodes for oxygen evolution

Pankaj Chauhan*[a], Basant Lal[b] & Smita Tung[c]

[a] Department of Chemistry, Faculty of Basic and Applied Sciences, Madhav University, Sirohi 307 026, Rajasthan, India

[b] Department of Chemistry, Institute of Applied Sciences and Humanities, GLA University, Mathura 281 406, India

[c] Department of Civil Engineering, GLA University, Mathura 281 406, India

E-mail: pankajc010198@gmail.com

Received 22 February 2025; accepted(revised) 24 March 2025

The ovalbumin sol-gel method has been used to manufacture the nano-sized spinel oxides Fe_3O_4, $NiFe_2O_4$, and $CuFe_2O_4$ at 550°C. These materials have then been characterized using the physicochemical Infrared (IR) spectrometry method with the (XRD) and electrochemical methods (CV), and Tafel polarisation. The IR and XRD have been used to establish the production of a stable spinel phase of metal oxides. IR spectra exhibits distinctive absorption bands at ~450 and ~586 cm^{-1} respective to the vibrations in octahedral and tetrahedral voids in spinel oxides. The development of nano-sized oxides with crystallite diameters of 28, 11, and 45 nm for pure, Ni, and Cu-ferrites has been verified by XRD powder patterns of decomposed oxide. The electrocatalytic performance for the oxygen evolution process has been investigated using the CV and Tafel polarization techniques in an alkaline medium on a fabricated GC/oxides/1MKOH electrode interface. Tafel slopes for (OER) at the higher over-potentials region ranges between (b = 118 –140 mV dec^{-1}) and follows almost first-order reaction mechanism and thermodynamic parameters such as the electrochemical activation energy ($\Delta H_{el}^{0\#}$) at constant potentials (0.85V) and the electrochemical entropy ($\Delta S^{0\#}$) for OER have also been estimated from the Arrhenius plot, with observed values ranging from 6 to 39 kJ mol^{-1} and a highly negative value of entropy (($\Delta S_{el}^{0\neq}$) = –330 J deg^{-1} mol^{-1}), respectively.

Keywords: Cyclic voltammetry, Electrocatalysis, Oxygen evolution reaction, Spinel oxide, Tafel Polarization

The fast expansion in human population put a lot of strain on energy demand and consumption. People use energy in a variety of ways throughout their day. The vast bulk of it is generated by the combustion of finite fossil fuels and takes the form of electrical energy. Because fossil fuel combustion emits considerable volumes of carbon dioxide into the atmosphere, which is linked to a wide range of ecological problems, it is vital to find alternative energy sources to minimize our dependency on fossil fuels. An effort has been made to develop certain oxide (Fe_3O_4, $NiFe_2O_4$, and $CuFe_2O_4$) materials for the more cost-effective formation of H_2 and O_2 utilized as green fuels to reduce our reliance on fossil fuels. In medical science, non-toxic oxides are used as an MRI contrast agent instead of gadolinium-based contrast agents and are used for treating anaemia following chronic kidney disorder[1]. Spinel structure transition metal mixed oxides (*e.g.* Fe_3O_4, $NiFe_2O_4$, and $CuFe_2O_4$) are considered very promising electrode materials for various applications in magnetic and biosensors, electrochemical energy devices (batteries, capacitors), information storage devices, and electrocatalysis[2-6], gas sensors[7], multilayer chip inductor[8], *etc.* and also as electrode material in the production of O_2, Cl_2chlorates, H_2 evolution, and O_2 reduction, etc[9]. Metal-substituted oxides are used as catalysts in a variety of processes, including the Haber Process[10] to create NH_3 and the breakdown of H_2O_2[11]. Spinel ferrite nanoparticles with metal substitutes are used for catalytic organic synthesis and dopamine analysis[12–15]. Co-precipitation[16], sonochemical method[17], hydrothermal[18], sol-gel process[19,32], citrate precursors method[20], microemulsion precursors techniques[21], a microwave-assisted method[22], and egg white sol-gel auto-combustion route[23] are just a few of the methods used to create these oxide materials. All of the methods for making metal-substituted ferrite (Fe_3O_4, $NiFe_2O_4$, and $CuFe_2O_4$) are relatively simple to use, favourable to the environment, and less expensive to produce when using sol-gel auto-combustion methods.

Egg-white precursors include a variety of proteins, including (ovalbumin, ovomucin, and globulin). The egg white precursor has a high nutritional content and

an excellent gelling and foaming character[24]. Along with the metal ions, these egg-white proteins completely dissolve in water to produce the amalgam foam. Ovotransferrin, one of the proteins found in egg whites, has a strong ability to bind metal ions. Glycoprotein ovotransferrin belongs to the transferrin family, which is well-known for its capacity to bind and transfer metal ions in the work described here, we synthesized pure and metal-substituted ferrites utilizing egg-white precursors using the sol-gel approach to characterize their physicochemical properties (IR, XRD), as well as the electrochemical activity towards OER in a solution of 1M KOH. Getting to low-cost, active, and fairly, particularly in alkaline solutions, transition metal mixed oxide of spinel (*e.g.* Fe_3O_4 and its Ni and Cu-substituted derivatives) are considered to be promising electrode materials for a variety of applications. As oxygen anode in alkaline water electrolysis, as an oxygen cathode in fuel cells and metal-air batteries, as an electrocatalyst in electroorganic synthesis, as a heterogeneous catalyst in catalytic converters (automobiles), *etc.* are a few significant applications that are anticipated. However, the specific surface area of these oxides made using traditional ceramic high-temperature methods is often low, and hence of low electrocatalytic activity. The interfacial surface properties of an oxide catalyst are known to play a key role in heterogeneous catalysis in general and in electrocatalysis in particular and depend greatly upon the oxide preparation variables such as methodology, precursors, and experimental conditions *e.g.* concentrations, *p*H, temperature, *etc.* To enhance surface area as well as electrocatalytic activity, these oxides have been prepared by low-temperature egg-white as precursor sol-gel route.

Experimental Section

The sol-gel technique was used to create nano-sized spinel-type oxides such as (Fe_3O_4, $NiFe_2O_4$, and $CuFe_2O_4$). This section required some chemicals such as iron nitrate (Merck, 99%), copper nitrate (Merck, 99.9% and nickel nitrate (Merck, 99.9%) AR grade, which were mixed in the stoichiometric ratio into 20 ml of double distilled water, and also prepared egg white solution in 30 ml of double distilled water and continuously stirred the solution before adding the metal nitrate solution. This produced solution was continually agitated at a temperature of 25°C until it became homogenous. To obtain the fluffy bulk powder, the resulting solution was evaporated at 100°C. This powder was transformed into nanoparticles of metal-substituted oxide by heating it to 550°C in a muffle furnace and then storing it in a desiccator. The required oxide sample was manufactured using the aforesaid procedure. FT-infrared spectroscopy and X-ray powder diffraction validated the production of oxide samples. Using an IR Affinity-1Shimadzu spectrophotometer to record the IR spectra of oxides in the wavenumber region 400 to 4000 cm^{-1} in KBr medium and XRD powder pattern of oxide samples were recorded using Cu-K-radiation, 1.54059 Å.

Verifying oxide's electrocatalytic activity for the OER, prepared oxides were transferred into the electrode either by depositing oxide onto the pre-treated glassy carbon electrode or by painting oxide slurry onto the one surface of the pre-treated glassy carbon. Electrochemical activity for OER in an alkaline medium, oxide electrodes were studied by the CV, LSV, and Tafel polarization techniques. The results of the aforementioned investigations show that using appropriate low-temperature preparation techniques, such as chemical or sol-gel types, can greatly improve the roughness and, consequently, the oxide catalysts' electrocatalytic activity. In the realm of material synthesis, the application of sol-gel technologies is currently gaining more and more attention. The latter technique often yields nano-crystalline ultrafine particles with significantly increased surface area at low preparation temperatures. Despite being intriguing from an electrocatalysis perspective, the sol-gel technique has not received much attention. Given the above, the base oxide, Fe_3O_4 of the spinel family was chosen and synthesized by two novel preparative methods, egg-white sol-gel to improve their electrocatalytic properties. Using TGA FTIR, XRD, SEM, CV, and Tafel polarization techniques, base oxide, and their substituted products were then examined for their electrochemical and physicochemical characteristics in context with the evolution of O_2 in a basic media.

Results and Discussion

FTIR

The sample was investigated by IR in a KBr medium with a wave number range of 400 to 4000 cm^{-1} to confirm the oxide formation. In all cases (Fe_3O_4, $NiFe_2O_4$, and $CuFe_2O_4$), the IR spectra showed typical peaks between 450 cm^{-1} and 586 cm^{-1}

wavenumber region corresponding to the metal-oxygen stretching mode of vibration in octahedral and tetrahedral crystals, respectively. The IR spectra shown in Fig. 1 shows some additional peaks which are 1120, 1368, 3534, 1530 & 1629 cm^{-1} due to the ascribed stretching vibration Fe^{3+}- O^{2-} in the tetrahedral void, carboxylate ion, symmetrical stretching vibration of O-H and scissoring vibration from water.

XRD

Oxide samples were produced at 550°C for 5 hours, and then their XRD powder patterns were studied between phage angle (2θ) 20-80 degrees. The formation of nano-sized spinel phage crystalline oxide is revealed by the powder's XRD pattern, as seen in Fig. 2. For pure, Ni-, and Cu-substituted ferrites, the XRD powder pattern exhibited peaks that match the planes (111), (220), (311), (222), (400), (422), (511), (440), (620), and (444) and are matched with their respective peaks given in the JCPDS Files (330-664, 74-2081, and 48-1548). XRD spectra showed the existence of a few smaller additional peaks indicating the production of Fe_2O_3 in small quantities along with the spinel. The crystallite size is determined by the Scherer formula ($S = \frac{0.9 \times \lambda}{\beta \cos\theta}$), where θ is Bragg angle, β is the Full Width At Half Maximum (FWHM), and S is the crystallite size of particles. Fe_3O_4, $NiFe_2O_4$, and $CuFe_2O_4$ have estimated sizes of ~53, ~11, and ~43 nm, respectively. These unique nanoscale crystallite particles demonstrated the nanoscale nature of the metal-substituted ferrite produced by the sol-gel process utilizing egg white as a precursor[22,23,25,26].

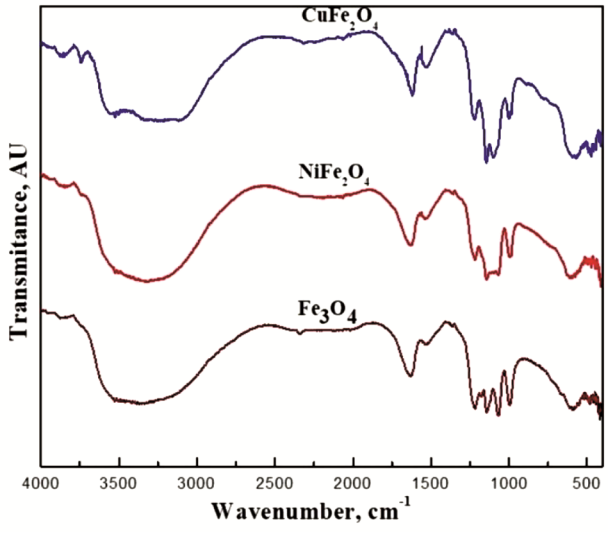

Fig. 1 —FTIR spectra of oxides prepared at 550°C: (a) Fe_3O_4 (b) $NiFe_2O_4$ and (c) $CuFe_2O_4$

Cyclic voltammetry (CV)

To establish the oxidation and reduction nature of the metal-substituted ferrite/KOH solution interface, the CVs of each metal-substituted ferrite electrode were measured in the potential range 0 to 0.7 V in 1 M KOH solution at 20 mV s^{-1}. Cyclic voltammograms of the GC/Fe_3O_4, GC/$NiFe_2O_4$, and GC/$CuFe_2O_4$ in the potential region of 0 to 0.7V do not exhibit redox peaks shown in Fig. 3. A similar type of cyclic voltammogram of Fe_3O_4 was additionally noticed on Ti support[27]. CV curve of $NiFe_2O_4$ oxide electrode shows a higher value of current densities (I_a) in comparison to Cu-substituted and pure ferrites on GC electrodes.

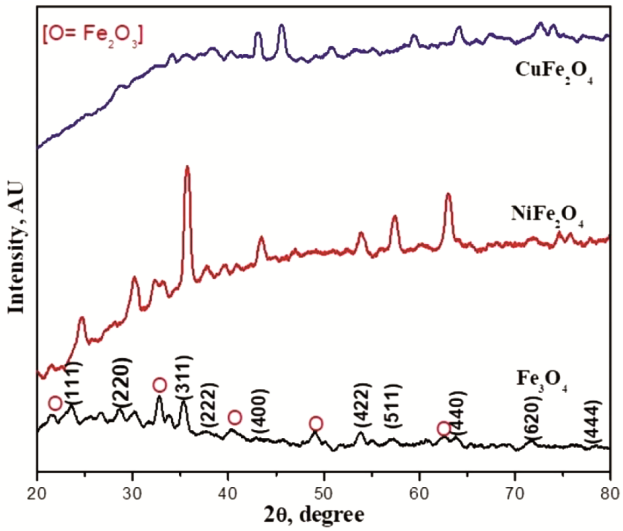

Fig. 2 — XRD powder patterns of oxides prepared at 550°C. (a) Fe_3O_4 (b) $NiFe_2O_4$ and (c) $CuFe_2O_4$

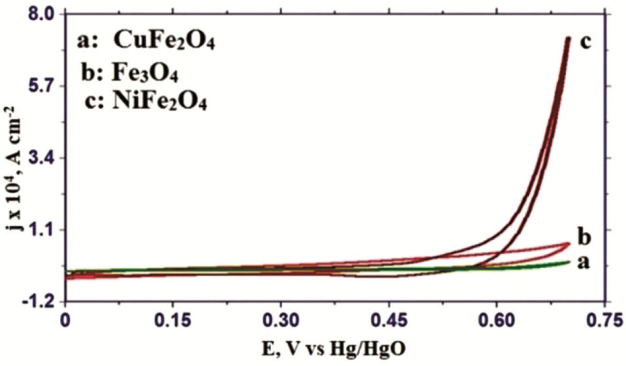

Fig. 3 —Cyclic voltammetric curves at 20 mV s^{-1} of (a) $CuFe_2O_4$ (b) Fe_3O_4 and (c) $NiFe_2O_4$electrodesat 25°C in 1 M KOH.

Roughness factor (R_F)

The oxide roughness factors were determined by recording cyclic voltammetry at several scan rates (10, 20, 40, 60, 80, and 100 in 1M KOH at 25°C in the potential region, 0.075-0.125 V) for each oxide electrode. Fig. 4a & 4b display a plot of charging current density *versus* scan rate and an example cyclic voltammogram of GC/$NiFe_2O_4$ electrodes at various scan speeds. The oxide/solution interface's double-layer capacitance (C_{dl}) was ascertained by analyzing the capacitive current (I_{cap}) *vs* scan rate slope. The Cdl of the smooth oxide electrode surface was assumed to be equal to 60 µF to determine the roughness factor for each oxide electrode[28,29]. The roughness value for (Fe_3O_4, $NiFe_2O_4$, and $CuFe_2O_4$) is 6 ±1. This indicated that there is no appreciable change observed in oxide roughness factors due to the metal substitution in the oxide matrix.

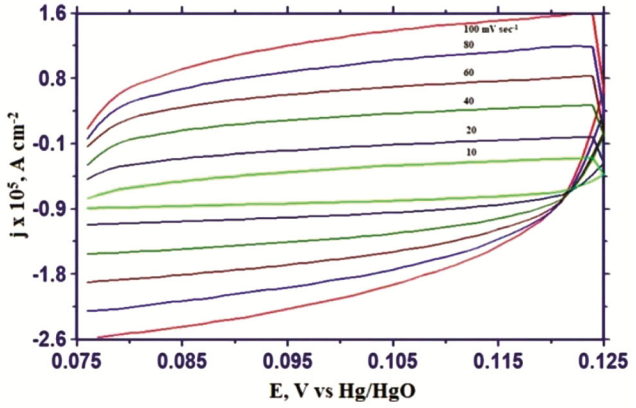

Fig. 4(a) — Cyclic voltammograms of the GC/$NiFe_2O_4$ electrode in a 1M KOH solution at 25°C at various scanning rates.

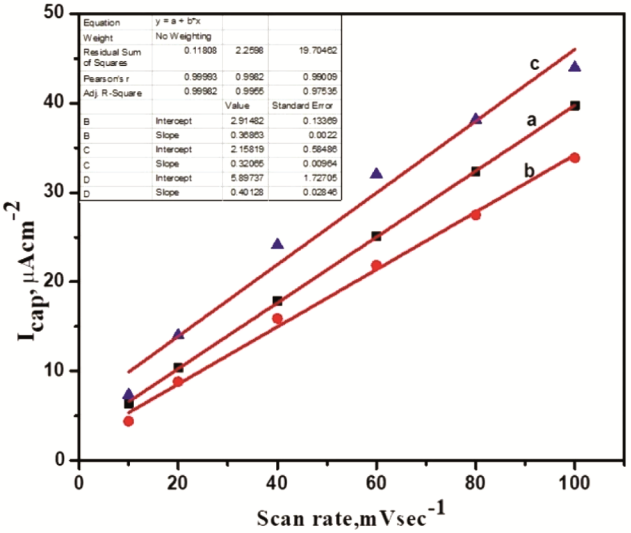

Fig. 4(b) — Plot of scan rate *versus* charging current density of (a) Fe_3O_4 (b) $NiFe_2O_4$, and (c) $CuFe_2O_4$ electrode at 25°C.

Tafel plot

The electrocatalytic performance of OER on pure base, nickel, and copper substituted ferrite electrodes were studied by recording an IR-free Tafel polarization curve at 25°C in a 1 M KOH solution as shown in Fig. 5, and observed data were given in Table 1. Considering the pure base, substituted oxides of nickel and copper, the measured Tafel slopes were 140, 124, and 118, respectively. With increased electrocatalytic activity, the metal-substituted oxide lowers the Tafel slope value, and $NiFe_2O_4$ exhibits a comparatively higher reduction. The electrocatalytic performance of the oxide electrode was also determined in terms of current density (*I*), either true current density (i_{tr}) or apparent current density (i_{app}) at fixed applied potentials (E) =850 mV. Both nickel and copper substitution in Fe_3O_4 marginally increased the electrocatalytic activity for OER. The electrocatalytic activity related to the conversion in the magnetic and electronic prospects of the ferrite catalyst is increased by the substitution of metal ions in the oxide matrix[29]. Both Orehotskey *et al.*[30] and Iwakura

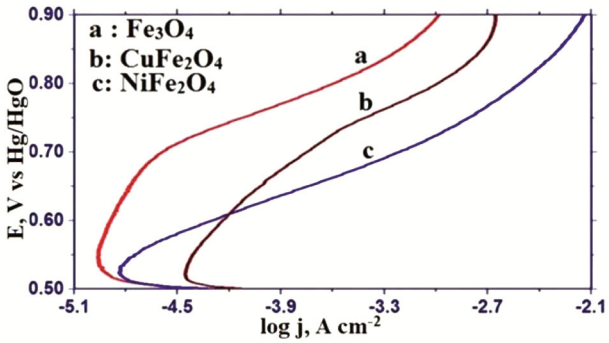

Fig. 5 — Tafel polarization curves on GC/metal substituted ferrites electrodes at 25°C in 1 M KOH: (a) Fe_3O_4 (b) $NiFe_2O_4$ and (c) $CuFe_2O_4$

Table 1 — Electrode kinetic parameters for OER on GC/ Fe_3O_4, $NiFe_2O_4$, and $CuFe_2O_4$ electrodes in 1M KOH at 25°C.

Oxide	Tafel slope(mV decade^{-1})	E/mV atI/mAcm^{-2}	I (mAcm^{-2})at E =850 mV			C_{dl} (mF)	R_F
	b	0.1	1.0	i_{app}	i_{tr}		
Fe_3O_4	140	761	894	0.624	0.104	360	6
$NiFe_2O_4$	124	628	724	5.209	0.982	320	5.3
$CuFe_2O_4$	118	653	799	1.862	0.282	400	6.6

et al.[31,32] also observed increases in electrocatalytic activity by nickel and copper substitution in ferrite matrix and magnetization saturation arising at room temperature. They also observed that the oxygen evolution process performs more electrocatalytically when the Bohr magneton is raised.

Order of reaction

The order of reaction (p) was calculated using the slope of the log i *vs* log [OH^-] plot displayed in Fig. 6 at a fixed potential (0.8 V) on the GC/oxide/KOH solution. This was performed by recording an IR-free Tafel polarization curve at various KOH concentrations (0.1 to 1.5M) with the ionic strength of medium constant (=1.5) by inert electrolyte KNO_3 on the GC of each oxide electrode. The order of reaction (p) for OER was observed to be unity. A similar order of reaction of oxygen evolution reaction was also reported elsewhere[33,34].

Activation energy

Thermodynamic parameters such as entropy of the reaction ($\Delta S^{0\#}$) and electrochemical activation energy ($\Delta H_{el}^{0\#}$) of fabricated electrodes for OER were measured by recording Tafel polarisation curves in 1M KOH solution at varying temperatures. The electrochemical activation energy ($\Delta H_{el}^{0\#} = -slope \times 2.303\,R$) was estimated through the Arrhenius plot's slope (logi *vs* 1/T) as displayed in Fig. 7 and the charge transfer coefficient (α) and standard activation energy($\Delta H_c^{0\#}$) were estimated from the value of Tafel slope (b) and different temperatures by using the equation ($\Delta H_c^{0\#} = \Delta H_{el}^{0\#} - \alpha FE$), respectively. The calculated values of $\Delta H_c^{0\#}, \Delta H_{el}^{0\#}$ *and* α are given in Table 2. The standard entropy of the reaction ($\Delta S^{0\#}$) is also calculated with the use of the following relation.

$$\Delta S^{0\#} = 2.303R\,[\frac{\Delta H_{el}^{0\#}}{2.303RT} + \log I - \log nF\omega C_{OH^-}]$$

where, $\omega = \frac{kT}{h}$ and n = 2 and other terms employed in the equation are understood as they normally would. Table 2 shows the electrochemical activation energy's value is reduced with the nickel and copper substitutions and also favors the increase of electrocatalytic performance toward OER in an alkaline solution. The extremely negative quantity of the standard entropy of the reaction suggests that the electrochemical formation of oxygen occurs through the adsorption of the reaction intermediate on the oxide electrode.

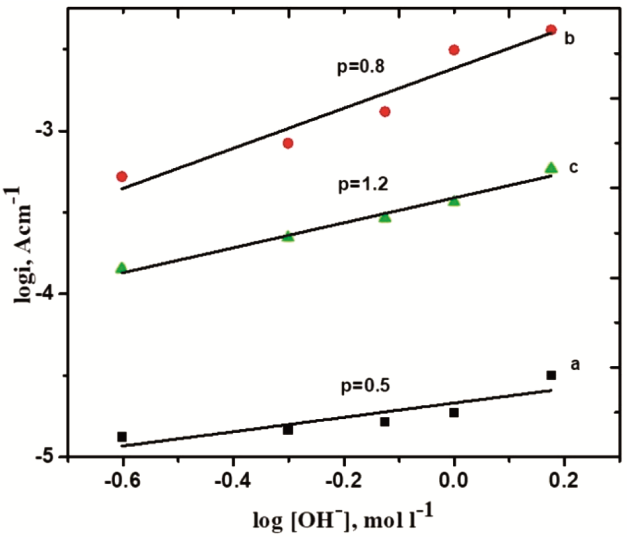

Fig. 6 — Plot of log i *vs* log [OH^-] at (E =0.8 V): (a)Fe_3O_4 (b) $NiFe_2O_4$ and (c) $CuFe_2O_4$

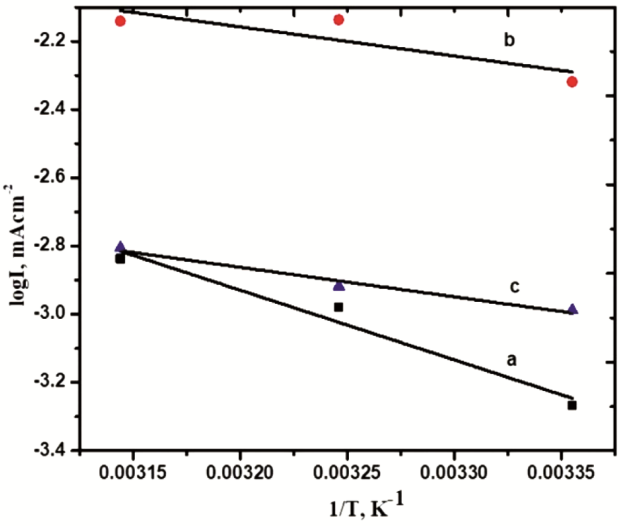

Fig. 7 — Arrhenius plots (logI *vs* 1/T) for GC/oxide electrodes: (a) Fe_3O_4 (b) $NiFe_2O_4$ and (c) $CuFe_2O_4$

Table 2 — Thermodynamic parameters for O_2 evolution on GC/Oxide electrode in 1M KOH

Electrode	$\Delta H_{el}^{0\neq}$ (KJ mol^{-1})at E = 0.84 V	$-\Delta S^{0\neq}$(J deg^{-1}mol^{-1})	α	$\Delta H_c^{0\neq}$(KJ mol^{-1})
Fe_3O_4	39	277	0.42	73
$NiFe_2O_4$	16.3	335	0.47	55
$CuFe_2O_4$	6.2	380	0.5	45

Conclusion

Pure base and nickel and copper substituted spinel oxides were prepared by a very simple and economical sol-gel method using egg white as a precursor. This method results in the formation of pure spinel phage oxides (*e.g.* Fe_3O_4, $NiFe_2O_4$, and $CuFe_2O_4$) with a high degree of crystallinity and nano-scale dimensions confirmed by the XRD. Fabricated oxide electrode was tested for their performance for OER in 1M KOH and found to be electrocatalytically active and it was improved considerably with the nickel substitution in the Fe_3O_4 matrix. These oxides can be useful for energy devices in the form of electrode materials and other several applications in different areas. The substitution of Fe in the Fe_3O_4 matrix with Ni and Cu greatly enhances the electrocatalytic activity of OER in a solution with alkaline conditions and significantly reduces the Tafel slope. The present work also raises the scientific community's attention to explore further investigation by developing similar or other oxide catalysts for several organic synthesis and remediation of eco-sensitive materials.

Future scope

Transition metal mixed oxide of spinel (*e.g.*, Fe_3O_4 and its Ni and Cu-substituted derivatives) are becoming affordable, fairly active, and, particularly in alkaline solutions, are thought to be promising electrode materials for a variety of applications. Some important applications that are predicted are as an oxygen anode in alkaline water electrolysis, as an oxygen cathode in fuel cells and metal-air batteries, as an electrocatalyst in electroorganic synthesis, as a heterogeneous catalyst in catalytic converters (automobiles), *etc*. Nevertheless, these oxides produced by conventional ceramic high-temperature techniques frequently have low specific surface areas, which results in low electrocatalytic activity. The oxides will be prepared using a precursor sol-gel method using low-temperature egg white to increase both surface area and electrocatalytic activity.

Acknowledgment

One of the authors, P. Chauhan, would like to express gratitude to Dr. M. Malviya of the Department of Chemistry at IIT BHU, Varanasi for providing the facilities required for electrochemical characterizations and to Prof. A. K. Tiwari of Babasaheb Bhimrao Ambedkar University, Lucknow, for giving the SEM of the oxide sample. The author additionally acknowledges the financial support provided by the Council of Science and Technology U.P. for the research project (CST/CHEM/D-1120 ID-1167). Author also acknowledges to Prof. Rajkumar Rana (Chairman) to providing invaluable facilities in Chemistry Lab at Madhav University

References

1 Shinde P, Rout C S, Late D P, Tyagi K, Singh M K, *Int J Hydrog Energy*,46 (2021) 2617.
2 Soloveichik G, *Nat Cat*, 2 (2019) 377.
3 Cheng F.Y, Su C H, Yang Y, Yeh S.C, Tsa C Y & Wu C L, *Biomaterial*,26 (2005) 729.
4 Song Q & Zhang Z J, *J Am ChemSoc,* 126 (2004) 6164.
5 Goldman A, *Modern Ferrite Technology*, (Springer, New York) 2006.
6 Niasari M S, Davar F & Mahamoudi T, *Polyhedron*, 28 (2009) 1455.
7 McMichael R D, Shull R D, Swartzendruber L J, Bennett L H & Wat-Son R E, *J MagnMagn Mat*, 111 (1992) 29.
8 Krishnaveni T, RajiniKant B V, Raju S R & Murthy S R, *J Alloys Comp*, 414 (2006) 282.
9 Trasatti S & Lodi G, *Electrodes of Conductive Metallic Oxides Part B*, (Trasatti Elsevier, Amsterdam) 1981, p 569.
10 Rajaram R R& Sermon P A, *J ChemSoc Faraday Trans: PhyChem Cond Phases*, 81 (1985) 2577.
11 Costa H M, Katan T, Chin M &Schoenweis J F, *Nature*,203 (1964) 1281.
12 Kumar Y, Vashishtha V K, Singh P P, Kumar A & Das D K, *Biointerface Res ApplChem*, 10 (2020) 5855.
13 Kumar Y, Singh P P, Pramanik P & Das D, *J SciInd Res*, 78 (2019) 177
14 Bansal S, Kumar Y, Das D K & Singh P P, *ChemChem Tech*, 2 (2019) 163.
15 Pippal P & Singh P, *Asian J SciTechnol*, 9 (2018) 7286.
16 Kim Y I, Kim D & Lee C S, *Phy B: Cond Matt,* 337 (2003) 42.
17 Shafi K V P M, Gediankem A &Prozorov R, *Chem Matt,* 10 (1998) 3445.
18 Bockris J O M &Otagawa T, *J PhysChem*,87 (1983) 2960.
19 Svegl F, Orel B, Svegl I G & Kaucic V, *ElectrochimActa*, 45 (2000) 4359.
20 Panda R N, Gajbhiye N S & Balaji G, *J Alloys Compd*, 326 (2001) 50.
21 Ahn Y, Choi E J, Kim S, Ok H N, *Mater Lett*, 50 (2001) 47.
22 Lal B &Rastogi P K, *Orbital: Elect J Chem*, 12 (2020) 154.
23 Senthil S M, Jayaprakash R, Singh V N, Mehta B R & Govindaraj G, *J Nano Res*, 4 (2008) 107.
24 Mine Y, *Trends Food Sci Technol*, 6 (1995) 225.
25 Panchal R M, Madhuri W, Shadhana K, Kim I G, Hul K N, Shiva Kumar K V & Rama Krishna R R, *J Sol-Gel Sci Technol*, 70 (2014) 400.

26 Singh N K, Yadav M K, Parihar R & Gangwar C, *J New Mat Electrochem Sys*, 23 (2020) 87.

27 Al-Hoshan M S, Singh J P, Al-Mayouf A M, Al-Suhybani A A & Shaddad M N, *Int J Electrochem Sci*, 7 (2013) 4959. Singh N K & Singh R N, *Ind J Chem*,38A (1999) 491.

28 O'Sullivan E J M &Calvo E J, *Comprehensive Chemical Kinetics Edited by R.G Comptom*, (Elsevier Amsterdam), 1987, p 274.

29 Orehotsky J, Huang H, Davison C R & Srinivasan S, *J Elec Chem*, 95 (1979) 233.

30 Iwakura C, Nishioka M & Tamura H, *Nippon Kagaku Kaishi*, 7 (1982) 136.

31 Iwakura C, Nishioka M & Tamura H, *Denki Kagaku*, 49 (1981) 535.

32 Chauhan P & Lal B, *J Electrochem Sci Tech*, 13 (2022) 497.

33 Lal B, *Indian J Chem*, 60A (2021) 1303.